A dual-center validation of the PIRAMD scoring system for assessing the severity of ischemic Moyamoya disease

Christiaan Hendrik Bas van Niftrik[1,2#], Martina Sebök[1,2#], Patrick Nicholson[3], Leonardo Olijnyk[4], Patrick Thurner[2,5], Lashmi Venkatraghavan[6], Joanna Schaafsma[7], Ivan Radovanovic[4], Joseph A. Fisher[6,8], Timo Krings[3,9], Zsolt Kulcsár[2,5], Michael Tymianski[4], Luca Regli[1,2], David J. Mikulis[9], Jorn Fierstra[1,2,4]

[1]Department of Neurosurgery, University Hospital Zurich, University of Zurich, Zurich, Switzerland; [2]Clinical Neuroscience Center, University Hospital Zurich, Zurich, Switzerland; [3]Division of Neuroradiology, Toronto Western Hospital, University of Toronto, Toronto, ON, Canada; [4]Division of Neurosurgery, Toronto Western Hospital, University of Toronto, Toronto, ON, Canada; [5]Department of Neuroradiology, University Hospital Zurich, University of Zurich, Zurich, Switzerland; [6]Department of Anesthesia and Pain Management, University Health Network, Toronto, ON, Canada; [7]Department of Neurology, Toronto Western Hospital, University of Toronto, Toronto, ON, Canada; [8]Institute of Medical Science, University of Toronto, Toronto, ON, Canada; [9]Joint Department of Medical Imaging and the Functional Neuroimaging Laboratory, University Health Network, Toronto, ON, Canada

Contributions: (I) Concept and design: CHB van Niftrik, M Sebök, J Fierstra; (II) Administrative support: CHB van Niftrik, M Sebök, DJ Mikulis, L Regli, J Fierstra; (III) Provision of study materials or patients: CHB van Niftrik, M Sebök, P Nicholson, L Olijnyk, P Thurner, L Venkatraghavan, JA Fisher, M Tymianski, L Regli, DJ Mikulis, J Fierstra; (IV) Collection and assembly of data: CHB van Niftrik, M Sebök, J Fierstra; (V) Data analysis and interpretation: All authors; (VI) Manuscript writing: All authors; (VII) Final approval of manuscript: All authors.

#These authors contributed equally to this work.

Correspondence to: Christiaan Hendrik Bas van Niftrik, MD, PhD. Department of Neurosurgery, University Hospital Zurich, Frauenklinikstrasse 10, 8091 Zurich, Switzerland; Clinical Neuroscience Center, University Hospital Zurich, Zurich, Switzerland. Email: bas.vanniftrik@usz.ch.

Background: Prior Infarcts, Reactivity, and Angiography in Moyamoya Disease (PIRAMD) is a recently proposed imaging-based scoring system that incorporates the severity of disease and its impact on parenchymal hemodynamics in order to better support clinical management and evaluate response to intervention. In particular, PIRAMD may have merit in identifying symptomatic patients that may benefit most from revascularization. Our aim was to validate the PIRAMD scoring system.

Methods: Patients with ischemic Moyamoya disease, who underwent catheter angiographic [modified Suzuki Score (mSS) and collateralization status], morphological MRI and a parenchymal hemodynamic evaluation with blood oxygenation-level dependent cerebrovascular reactivity (BOLD-CVR) at two transatlantic centers, were retrospectively included. The primary outcome was the presence of neurological symptoms. The diagnostic capacity of each PIRAMD feature alone was evaluated, as well as combined and the inter-institutional differences of each parameter were evaluated.

Results: Seventy-two hemispheres of 38 patients were considered for analysis, of which 39 (54%) were classified as symptomatic. The presence of a prior infarct had the highest odds ratio [odds ratio (OR) =24; 95% CI: 6.7–87.2] for having neurological symptoms, followed by impaired CVR (OR =17; 95% CI: 5–62). No inter-institutional differences in the odds ratios or area under the curve (AUC) were found for any study parameter. The PIRAMD score had an AUC of 0.88 (95% CI: 0.80–0.96) with a similar AUC for the PIRAMD grading score.

Conclusions: Our multicentric validation of the recently published PIRAMD scoring system was highly effective in rating the severity of ischemic Moyamoya disease with excellent inter-institutional agreement. Future studies should investigate the prognostic value of this novel imaging-based score in symptomatic patients with Moyamoya disease.

Introduction

Moyamoya disease is a cerebrovascular steno-occlusive disease often resulting in a progressive stenosis of one or both supraclinoidal segments of the internal carotid artery (ICA) and its proximal branches, promoting development of subsequent fine collaterals—known as Moyamoya collaterals (1,2). Surgical revascularization of the symptomatic hemisphere is a well-studied and effective treatment option in patients with Moyamoya disease and ischemic symptoms, however, the risks associated with the treatment mandate careful patient selection (3-7). Ideally, such selection should be supported by multimodal structural and hemodynamic imaging, in order to better inform about subsequent stroke risk that can be weighed against the operative risks (8-10). Current standard clinical imaging only incorporates structural imaging and potentially a steady-state hemodynamic imaging like dynamic susceptibility contrast magnetic resonance (MR) perfusion, which could severely underestimate the extend of disease. And only a few centers have routine access to dynamic cerebral hemodynamic perfusion imaging.

A novel imaging-based scoring system assessing the severity of disease and its impact on parenchymal hemodynamics has been proposed by Ladner and colleagues (11). The scoring system is based on the combination of prior infarctions, impaired cerebrovascular reactivity (CVR) in the anterior flow territory using blood oxygenation-level dependent cerebrovascular reactivity (BOLD-CVR) and angiographic features in Moyamoya disease (PIRAMD: Prior Infarcts, Reactivity and Angiography in Moyamoya Disease). The benefit of this novel scoring system is that both the static MRI sequences and BOLD fMRI sequence are available on all MR scanners and DSA is a widely used imaging technique as well. Therefore, this could be applied worldwide as all three imaging modalities are widespread available.

The PIRAMD score can have great merit in structuring the diagnostic evaluation of patients with Moyamoya disease and identification of a subgroup of symptomatic patients that may benefit most from revascularization, or just as important, may provide further back support for a wait-and see routine including routine neurological investigations with repeated static and hemodynamic MR investigations in combination with medical treatment.

Although the PIRAMD scoring system shows promise for correlating hemodynamic impairment and symptomatic Moyamoya disease validation in an independent Moyamoya cohort has not been done. The purpose of this investigation was therefore to rate the PIRAMD scoring performance in two ischemic Moyamoya disease patient cohorts from independent transatlantic quaternary Moyamoya referral centers. This manuscript is presented in accordance with the TRIPOD reporting checklist (available at https://qims.amegroups.com/article/view/10.21037/qims-22-1062/rc).

Methods

Subject recruitment and assessment

University Hospital Zurich (UHZ), i.e., Zurich database
Patients with ischemic Moyamoya disease were retrospectively selected from an ongoing prospective BOLD-CVR database containing all patents with cerebrovascular steno-occlusive disease between October 2014 and April 2021. Prior to inclusion in the BOLD-CVR database, this study was approved by the ethics committee of University Hospital Zurich (KEK-ZH-Nr. 2012-0427 & KEK 2020-02314), and all patients signed an informed consent. Exclusion criteria for the BOLD-CVR database were: patients <18 years old, pregnant or breastfeeding women, patients with a contra-indication for magnetic resonance imaging, severe claustrophia, or patients with suffer from the following hearts disease: myocardial infection and a recent myocardial infarction, patients who suffer from the following pulmonary diseases: pneumonia, pneumothorax, pleura effusion and severe pulmonary insufficiency and last patients who suffer a venous vessel occlusion with or without a pulmonary emboli. All patients were medically treated according to the stroke protocols of both institutes, which included anti-thrombotic agents (primarily aspirin, unless the multiplate test showed that the patients were aspirin non-responders then clopidogrel was chosen) and statins.
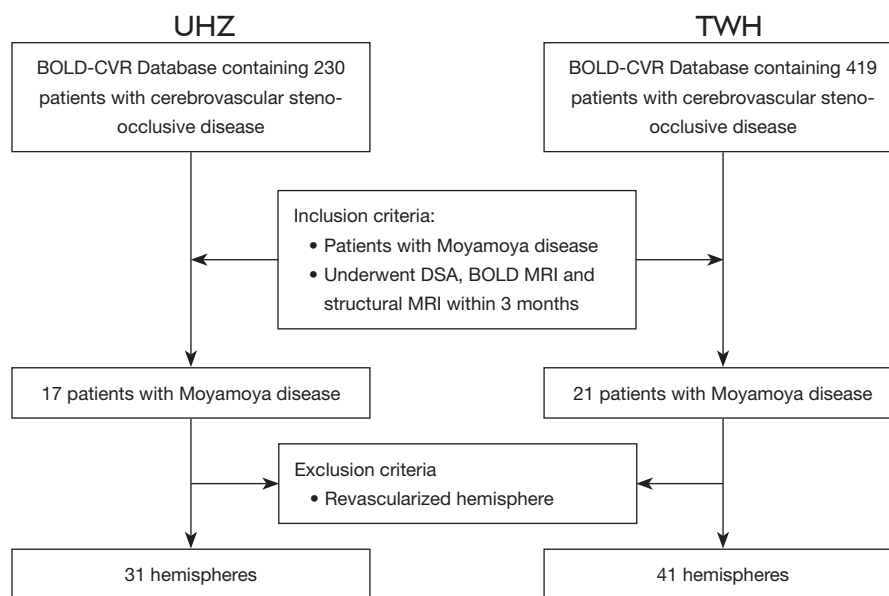
Figure 1 Patient inclusion flow chart. The flow chart depicts the patient inclusion and exclusion applied by both centers. UHZ, University Hospital Zurich; TWH, Toronto Western Hospital; BOLD-CVR, blood oxygenation-level dependent cerebrovascular reactivity; DSA, digital subtraction angiography; MRI, magnetic resonance imaging.

Toronto Western Hospital (TWH), i.e., Toronto database

Data of ischemic Moyamoya patients were retrospectively extracted from an ongoing prospective BOLD-CVR database between June 2005 and April 2021. This study was approved by the research ethics board (UHN REB #13-7168) at the University Health Network and all subjects provided informed consent before inclusion. The exclusion criteria form the BOLD-CVR database are similar to those described above.

Inclusion and exclusion criteria

All patients who underwent both, a diagnostic digital subtraction catheter angiography (DSA) and a BOLD-CVR within 3 months, were included. Patients with novel symptoms in the interval between the DSA and the BOLD-CVR scan, patients with either unilateral or bilateral cerebrovascular EC-IC bypasses for symptomatic Moyamoya disease were excluded. In patients with bilateral Moyamoya disease and a unilateral cerebral bypass, only the non-treated hemisphere was evaluated. A flow-chart describing the patient inclusion and exclusion is presented in *Figure 1*. The study was conducted in accordance with the Declaration of Helsinki (as revised in 2013).

Imaging parameters

THE Diffusion Weighted, FLAIR-weighted and T2-weighted imaging were obtained from the routine clinical imaging protocol on a 3.0T scanner (Zurich-Skyra, Siemens, Erlangen, Germany-Zurich or Ingenia-Phillips, Philips Healthcare, Best, Netherlands) and (Toronto: Signa HDX platform, GE Healthcare, Milwaukee, Wisconsin, USA) as applied on a daily basis in both centers. These imaging protocols differed for each scanner and were slightly altered over the years. As the aim of this study was to validate the PIRAMD score, the slight differences in protocol and image quality were accepted, specifically as the images were of such quality, that they were used for clinical purposes.

The angiography in both centers obtained were all done transfemorally with the use of 5F catheters using an Arts Zee Interventional Angiography System (Siemens Healthcare GmbH, Erlangen, Germany). With the use of selected 8 mL injections of non-ionic contrast (Optiray 300, Guerbet, France), anteroposterior and lateral views of both the internal carotid arteries and both vertebral arteries were obtained.

All BOLD fMRI scans were performed on a 3.0T scanner

(Skyra, Siemens, Erlangen, Germany) with a 32-channel phased array head coil. BOLD MR CVR parameters: T2*-weighted echoplanar gradient-echo sequence (TR 2,000 ms, TE 30 ms, flip 85°, 3 mm isotropic voxels, 200 temporal frames). A high-resolution 3-dimensional T1-weighted image with the same orientation as the BOLD fMRI scans: 0.8×0.8×1.0 mm with a field of view 230×230 mm and resolution of 288×288, 176 slices per slab with a thickness of 1 mm, repetition time/echo time 2,200/5.14 ms, inversion time 900 ms, and flip angle 8°.

Toronto

All MRI scans were performed on a 3.0T scanner (Signa HDX platform, GE Healthcare, Milwaukee, Wisconsin, USA) with an 8-channel phased array head coil. BOLD MR CVR parameters: T2*-weighted echoplanar gradient-echo sequence (TR 2,000 ms, TE 30 ms, flip 85°, voxel size range 3.75×3.75×5 mm to 3 mm isotropic, no gap, field of view 24×24 cm, matrix 64×64, 255 temporal frames). A high resolution T1-weighted image as anatomical correlate was done using the following parameter: 1.0 mm thick, matrix 256×256, field of view 22×22 cm.

Evaluation of the 4 PIRAMD parameters

Prior infarction

Following Ladner *et al.* (11), all hemispheres were evaluated separately. Prior infarctions were present if (I) diffusion Weighted Imaging lesions could be seen in prior MRI images, or (II) based on FLAIR and T2 weighted imaging acquired around the time of the BOLD-CVR scan. For lacunar infarcts, a size criterion for hyperintense lesions on both FLAIR-weighted and T2-weighted imaging with greatest axial diameter ≥4 mm was used to separate prior infarcts from white matter changes. As this method evaluates both acute and chronic infarctions, no time limit was set between infarct onset and diagnosis.

Evaluation of hemodynamics with noninvasive BOLD fMRI to assess CVR

CVR describes the response of a vascular bed as a reaction on the presence of a vasoactive stimulus and is a wide-spread used parameter to evaluate cerebrovascular health (12). Although usually obtained using Positron-Emission-tomography in combination with a nuclear tracer, BOLD functional imaging in combination with a CO_2 stimulus has shown its good capacity to evaluate CVR (BOLD-CVR)

without the need for radiation (13). BOLD-CVR is defined as the % BOLD fMRI signal change/mmHg CO_2 change.

Similar to Ladner *et al.* (11), in this study BOLD-CVR was obtained through a hypercapnic stimulus (14-17). At both institutes, the hypercapnic stimulus was given by a custom-build computer-controlled gas blender [RespirAct™, Thornhill Research Institute, Toronto, Canada—for more specifics on the specs necessary for the RespirAct, see Slessarev *et al.* (18)]. This standardized procedure allows not only for a reproducible stimulus, but unlike Ladner *et al.* (11), a normoxic hypercapnic stimulus decreases unknown signal alterations due to a changing arterial partial pressure of oxygen (19).

Both centers used a predefined normoxic hypercapnic CO_2 stimulus applied using block protocol, specific for that center. In Zurich, the block protocol applied was a single block protocol, which includes a clamping of the subject on its resting CO_2 and O_2. After the 100 s of baseline imaging, an 80 second normo-oxic-hypercapnic stimulus is applied increasing the resting CO_2 with ~10 mmHg CO_2 (20). The investigation is ended with a second resting baseline imaging of 100 s.

In Toronto, the block protocol consists of two block protocols with an initial short normoxic challenge of 40 s and a secondary longer hypercapnic challenge of 110 s with returns to baseline breathing values before, between and after the hypercapnic challenges (21).

The BOLD fMRI and respiratory data are then taken from the scanner and Respiract and analyzed using in-house scripts. The fMRI images are preprocessed using slice-time correction, motion correction and smoothed with a Guassian Kernel of 6 mm.

After, BOLD-CVR is calculated on a voxel-by-voxel basis after delay correction using a linear regression analysis to obtain BOLD-CVR (% BOLD fMRI signal change/ mmHg CO_2) [for more information see van Niftrik *et al.* (19) and Sobczyk *et al.* (12)].

CVR impairment was diagnosed if a significant region with steal phenomenon [i.e., paradoxical (= negative) BOLD-CVR response] was present in the anterior circulation (i.e., present in at least 1/3 of the anterior circulation) (22-25). This was determined by experienced neuroradiologists of each center separately.

This CO_2 stimulus and the connected CVR analysis method applied by both centers are different from Ladner *et al.* (11) as they applied the hyperoxic stimulus in a non-controlled setting which results in non-reproducible

measurements (16). However, as the aim of the current study was to evaluate the PIRAMD score independent of measurement methods of the separate imaging, it was deemed valid to defer from this specific original investigation protocol used by the primary investigators.

Angiographic evaluation

Following Ladner *et al.* (11), all angiographic features were independently evaluated by two neuroradiologists per center (Zurich: PT & ZK; Toronto: DM & PN). Moyamoya disease characteristics and severity on DSA were scored with a modified Suzuki Score (mSS), ranging from 0 to IV with higher grades representing more severe disease separately for each hemisphere (26). The mSS accounts for ICA, middle cerebral artery (MCA), and anterior cerebral artery disease, along with the presence or absence of lenticulostriate collaterals. As a secondary angiographic analysis, regional collateralization on DSA was assessed for 7 individual vascular anatomical regions of the middle cerebral artery territory, that was based on a modification of the Alberta Stroke Program Early CT Score (ASPECTS; i.e., M1 through M6 and basal ganglia) (27). This ASPECTS score modification and adaption for DSA for the PIRAMD score has been extensively explained in the initial paper by Ladner and colleagues (11). A vascular territory was considered impaired if there were no visible collateral vessels supplying the ischemic site or if there were collaterals only to the periphery of the ischemic site. Alternatively, a vascular territory was considered unimpaired if collateral blood flow provided complete perfusion to the vascular bed in a region with ischemia or if there was normal anterograde flow. The total number of impaired territories (0–7) was counted for each hemisphere.

For statistical analysis, each hemisphere was binarized based on the presence of absence of ≥2 impaired territories. As it is a retrospective analysis, the neuroradiologists were not blinded to the outcome measurement.

Outcome measurement

All included hemispheres were binarized according to the presence or absence of a symptomatic hemisphere. Symptomatic hemispheres were defined as those with either a history of recurrent localizable transient ischemic attacks (TIAs) or persistent neurological deficits referable to the hemisphere. Like Ladner *et al.* (11), psychological symptoms, deficits in concentration and memory, and/or headache were not included, given the potential ambiguity in localization and therefore unknown classification

PIRAMD score and grade

Mimicking the methods by Ladner *et al.* (11), for each hemisphere a single PIRAMD Score as well as a PIRAMD Grade was calculated. The PIRAMD score was inferred from the four primary imaging parameters. For the presence of a Prior Infarct, 1 point was given, while the presence of impaired CVR, an mSS ≥2 and the presence of ≥2 impaired vascular territories were all rewarded three points. In the end, the sum of each a hemisphere could total up to a maximum of 10 PIRAMD points. The PIRAMD grading classified hemispheres based on the PIRMAD Score into Grade 1: PIRAMD score between 0–5; Grade 2: PIRAMD score between 6–9; Grade 3: PIRAMD score of 10.

Statistical analysis

All statistical analyses were performed using SPSS Statistics 26 (IBM Corp., Armonk, NY, USA).

All data was analyzed per center and combined. The baseline characteristics and the PIRAMD parameters were evaluated between the two cohorts using the Mann Whitney U-test.

The diagnostic capacity of each PIRAMD feature alone was evaluated using a binary Logistic regression and receiver operating curve (ROC) analysis. The ROC analyses were also repeated for PIRAMD score and grade. An inter-institutional difference analysis for the diagnostic capacity for all PIRAMD individual parameters was performed. The correlation between the PIRAMD scores and the presence of a symptomatic hemisphere was determined using the Spearman correlation coefficient. The bootstrapping technique presented by Ladner *et al.* (11) had been repeated to allow for an optimal comparison. Finally, we have applied a model calibration to the PIRAMD score and grade. This describes the ability of the model to produce unbiased estimates of the probability of the calculated outcome and was done by determining three factors: (I) the goodness of fit test as defined by the R^2 of the regression analysis, (II) the calibration of large (intercept of the model), where = indicates a perfect calibration and less or higher then = indicates and over or under-estimation of the outcome and (III) recalibration slope (slope of the model), which shows the average predictor effects. Here a value of 1 indicates a perfect agreement between the strengths of the predictors and validation data and a value less or more than 1 indicates a stronger or weaker predictor effect (28,29).

For all patients, all variables were available as the included investigations were part of the clinical routine. Therefore, we had no missing data in our patient population.

Results

After evaluating the inclusions and exclusion criteria (*Figure 1*), the Zurich database contained 17 patients and the Toronto database contained 21 patients applicable for further analysis. *Table 1* contains baseline characteristics and PIRAMD score parameters of the whole cohort and of both hemispheres separately. As for this study, only non-revascularized hemispheres were included, the final analysis comprised of a total number of 38 patients with 72 hemispheres of which 39 (54%) were classified as correlating to clinical symptoms to that hemisphere (i.e., affected or 'symptomatic' hemisphere). The mean age of included patients was 54 (range, 20–82 years) and 27 patients (71%) were female. The mean age of the Toronto cohort was higher than the Zurich cohort (P=0.01) and showed marked differences in the mSS (P=0.01) and the number of affected collaterals (P=0.03). The other variables were comparable between both centers. *Table 2* shows the outcome measurements of all different parameters evaluated in the paper. As compared to Ladner *et al.* (11), our patient characteristics and clinical data did not differ from their patient cohort, nor did the average number of symptomatic hemispheres [Ladner: 28 (60.9%) *vs.* 39 (54%); see *Table 1* for comparison].

Structural MRI data: prior infarctions

A prior infraction on T2-weighted FLAIR images was seen in 34 hemispheres (47%). The presence of a prior infarct strongly increases the odds of being symptomatic [OR 24 (95% CI: 7–87, P<0.001), *Table 2*]. The area under the curve (AUC) was 0.82 (95% CI: 0.72–9.3; *Table 2*, *Figure 2*) with no differences between both centers (AUC difference 0.154, P=0.14; *Table 2*).

Hemodynamic MRI data: quantitative BOLD-CVR

Of the total cohort, 46 (64%) hemispheres exhibited impaired CVR (= steal phenomenon). Hemispheres with impaired CVR had an odds ratio of 17 (95% CI: 5–62; *Table 2*) times greater to be symptomatic as compared to hemispheres without impaired CVR. In the ROC analysis, impaired CVR had an AUC of 0.80 (95% CI: 0.68–0.91, P<0.001; *Table 2*, *Figure 2*). For TWH, the AUC was 0.75 (95% CI: 0.59–0.915) and for UHZ 0.85 (95% CI: 0.69–0.99) without a significant difference between the AUC's (AUC difference −0.09, P=0.43; *Table 2*).

Angiographic data

An mSS ≥ Grade II was observed in 54 hemispheres (75%) and 43 hemispheres (60%) had 2–7 vascular territories impaired. The odds of having a symptomatic hemisphere with an mSS ≥ Grade II was increased by 10.0 (95% CI: 2.5–39.0, P=0.001; *Table 2*). Similarly, having ≥2 vascular territories impaired increased the odds ratio to 9.14 (95% CI: 3.0–27.3, P=0.003; *Table 2*). The AUC for mSS was 0.69 (95% CI: 0.56–0.82, P=0.006; *Table 2*, *Figure 2*) and 0.74 (95% CI: 0.63–0.86, P<0.001; *Table 2*, *Figure 2*) for the parameter impaired collaterals. Both parameters did not show a significant difference between both centers (mSS: AUC TWH: 0.71 *vs.* UHZ 0.65 with a non-significant difference 0.56, P=0.68; impaired collaterals: 0.43, P=0.54; *Table 2*).

Validation of the PIRAMD score and PIRAMD grade

Exemplary images of a patient from Zurich and Toronto can be found in *Figure 3*. An increase in PIRAMD score was strongly associated with the presence of a symptomatic hemisphere (rho =0.65, P<0.001). The AUC of the PIRAMD score for the whole cohort was 0.88 (95% CI: 0.80–0.96; *Table 2*, *Figure 2*) with an AUC of 0.88 (95% CI: 0.78–0.98; *Figure 2*) for the Toronto cohort, and an AUC of the 0.89 (95% CI: 0.78–1.0) for the Zurich cohort (AUC difference 0.006, P=0.94). The optimal cut-off point to discriminate between patients lies at a PIRAMD score of 6.5 (sensitivity of 0.92, specificity of 0.75). In comparison, the PIRAMD grade performed similar to the PIRAMD score (AUC 0.85; 95% CI: 0.76–0.94; *Figure 2*). Last, between all the parameters, as is expected, there is a co-linearity seen for all parameters, the highest values found between the two angiographic scores (rho =0.75, P<0.001) and between BOLD-CVR and the angiographic scores (CVR *vs.* mSS: rho =0.62, P<0.001; CVR *vs.* collaterals: rho =0.65, P<0.001). Both the PIRAMD score and PIRAMD grade performed well on the model calibration (*Figure 4A,4B*). The R^2 of PIRAMD score was 0.39 with a calibration-in-the-large value of 0.01 and a recalibration slop of 0.98, whereas the R^2 of the PIRAMD grade was 0.40 with a calibration-in-the-large of 0.003 and a recalibration slope of 0.99.

Discussion

The PIRAMD scoring system had been proposed by Ladner *et al.* (11) to classify ischemic Moyamoya disease

Table 1 Patient characteristics

Variables	Complete cohort (N=38)	Toronto (N=21)	Zurich (N=17)	P value*	Initial cohort by Ladner *et al.* (11) (N=25)
Available hemispheres	72	41	31	–	46
Age (years), mean [range]	54 [20–82]	57 [29–82]	49 [20–72]	0.01	42
Female	27 (71%)	17	10	0.01	20
Prior stroke	33 (46%)	20	13	0.56	30
CVR impairment	46 (64%)	28	18	0.26	35
Modified Suzuki Score				0.01	
0	13 (18%)	5	8		3
1	5 (7%)	2	3		5
2	20 (28%)	8	12		20
3	19 (26%)	14	5		14
4	15 (21%)	12	3		4
Affected collaterals				0.03	
0	24 (33%)	14	10		10
1	5 (7%)	2	3		1
2	7 (10%)	1	6		6
3	9 (13%)	3	6		10
4	13 (18%)	10	3		10
5	10 (14%)	7	3		3
6	4 (5%)	4	0		3
PIRAMD score				0.01	
0	12 (17%)	5	7		2
1	1 (1%)	0	1		2
3	8 (11%)	5	3		3
4	1 (1%)	0	1		1
6	6 (8%)	4	2		3
7	7 (10%)	6	1		7
9	13 (18%)	7	6		8
10	22 (31%)	14	8		20
PIRAMD grade				0.23	
1	22 (31%)	10	12		8
2	28 (38%)	17	11		18
3	22 (31%)	14	8		20
Symptomatic hemispheres	39 (54%)	24	15	0.40	28

*, P<0.05 was considered statistically significant. CVR, cerebrovascular reactivity; PIRAMD, Prior Infarcts, Reactivity, and Angiography in Moyamoya Disease.

Table 2 Outcome measurements

PIRAMD parameters	Odds ratio (symptomatic)	AUC	AUC difference TWH-UHZ
Infarct (95% CI)	24 (7–87, P<0.001)	0.82 (0.72–9.3, P<0.001)	0.154, P=0.14
BOLD-CVR (95% CI)	17 (5–62, P<0.001)	0.80 (0.68–0.91, P<0.001)	−0.09, P=0.43
mSS (95% CI)	10.0 (2.5–39.0, P=0.001)	0.69 (0.56–0.82, P=0.006)	0.56, P=0.68
Collateral (95% CI)	9.14 (3.0–27.3, P=0.003)	0.74 (0.63–0.86, P<0.001)	0.43, P=0.54

PIRAMD, Prior Infarcts, Reactivity, and Angiography in Moyamoya Disease; CI, confidence interval; BOLD, blood-oxygenation-level dependent; CVR, cerebrovascular reactivity; mSS, modified Suzuki Score; AUC, area under the curve (non-symptomatic *vs.* symptomatic); TWH, Toronto Western Hospital; UHZ, University Hospital Zurich.
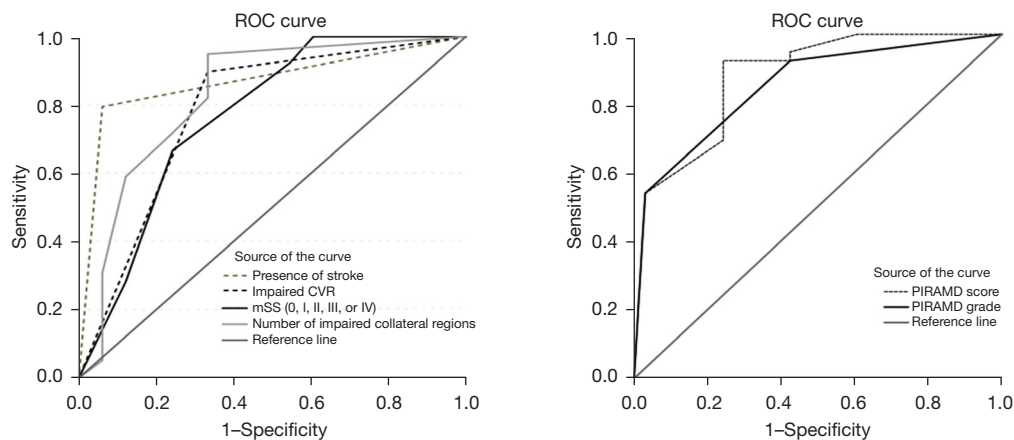
Figure 2 ROC curves of the PIRAMD parameters and outcome scores. ROC curve for each scoring parameter (left) of the combined dataset (n=72) and for both the PIRAMD score and the PIRAMD grade. ROC, receiver operating characteristic; CVR, cerebrovascular reactivity; mSS, modified Suzuki Score; PIRAMD, Prior Infarcts, Reactivity, and Angiography in Moyamoya Disease.

severity using structural and hemodynamic imaging data, to better support clinical management and evaluate intervention response. Our multicentric data also confirms the efficacy of PIRAMD in scoring the severity of ischemic Moyamoya disease with an excellent inter-institutional agreement and a good calibration of the PIRAMD score and grade. We have found that all individual imaging parameters composing the PIRAMD score, to strongly increase the odds for a symptomatic hemisphere with the total sum of the PIRAMD score being the best predictor with an AUC of 0.89. The diagnostic capacity of both angiography parameters were equal to findings by Ladner and colleagues (11), whereas the diagnostic capacity of prior infarct and impaired CVR combined, were on average higher than found by Ladner *et al.* (11). This could be due to a difference in patient selection. In our centers, only symptomatic patients were referred for further hemodynamic evaluation and, therefore, no patients with

an incidental Moyamoya diagnosis were included in this study. The diagnostic strength of the PIRAMD is indicated by its AUC of 0.88. The optimal PIRAMD cut-off point between asymptomatic and symptomatic hemispheres in our cohort was 6.5, comparable to 6.0 found by Ladner *et al.* This small difference appears to be due to the effect of the parameter 'prior infarctions' which had a much larger influence in our cohort. Last, the model seems to be very stable with no significant differences in the inter-institutional analysis despite the use of different MR vendors (i.e., 3-tesla Siemens for UHZ, and 3-tesla GE for TWH), a slightly different BOLD-CVR protocol and different interventional neuroradiological teams performing the angiographies.

Current evaluation systems of Moyamoya disease

As Moyamoya disease is a very rare disease, patients are

4626

van Niftrik et al. Validation of the PIRAMD score to assess Moyamoya severity
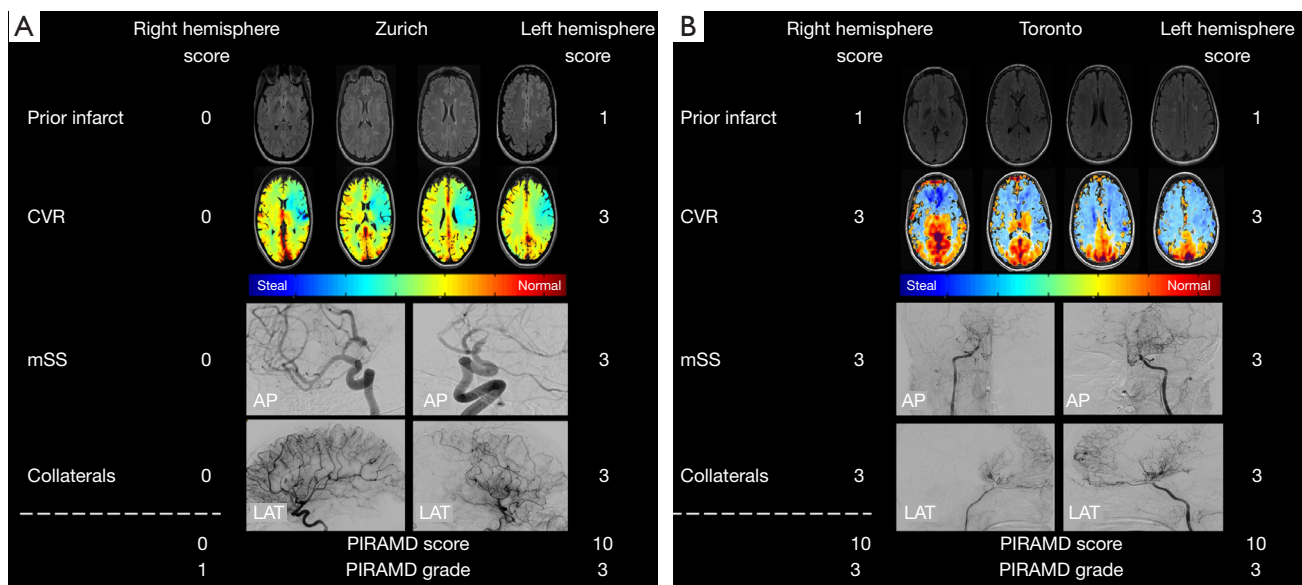
Figure 3 Illustration of PIRAMD scoring system for an individual patient from both centers. (A) An exemplary patient from the Zurich database where the PIRAMD scoring system is applied (i.e., prior infarct determination on T2-weigthed FLAIR MRI, determination of impaired cerebrovascular reactivity from BOLD fMRI CVR imaging, determining a modified Suzuki Grade Score, and assessment of the number of impaired collaterals on DSA using the modified APECTS score). With the presence of an prior infarction in the left hemisphere (1 point), the presence of negative (blue) BOLD-CVR in the anterior circulation (3 points) and the presence of an mSS >2 and the presence of impaired collateralization (both 3 patients), the patient obtained 10 points for his left hemisphere, while the contralateral hemisphere displayed none of these characteristics (0 points). (B) The determination of the PIRAMD Score for an individual patient from the Toronto database. These patients with Moyamoya disease displayed a bilateral disease and were classified with 10 patients for both hemispheres. CVR, cerebrovascular reactivity; mSS, modified Suzuki Score; AP, anterior-posterior; LAT, lateral; PIRAMD, Prior Infarcts, Reactivity, and Angiography in Moyamoya Disease; FLAIR, fluid attenuated inversion recovery; BOLD, blood-oxygenation-level dependent; fMRI, functional magnetic resonance imaging; DSA, digital subtraction angiography.
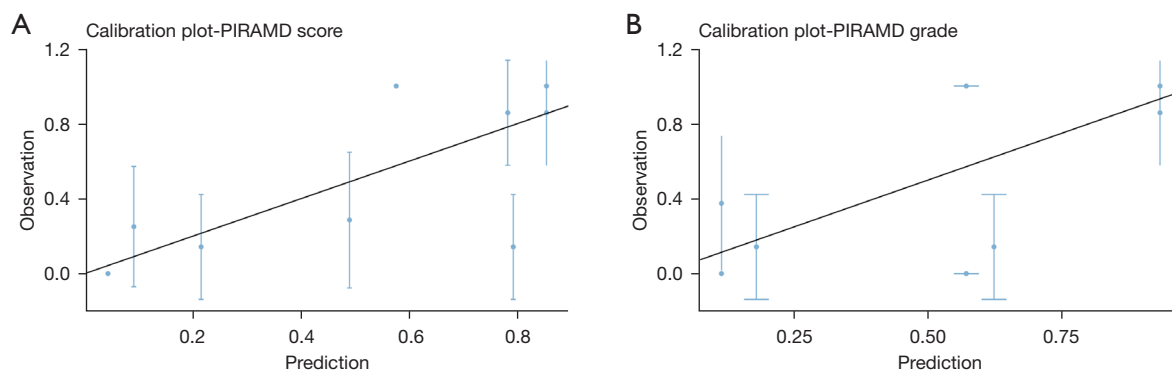
Figure 4 Calibration plots. Calibration plots for the PIRAMD score (A) and the PIRAMD grade (B) to predict the presence of a symptomatic hemisphere. PIRAMD, Prior Infarcts, Reactivity, and Angiography in Moyamoya Disease.

often quickly referred to an experienced center for further evaluation and treatment of the disease. Such evaluation is usually done based on a standard battery of test in

combination with the discretion of the treating physical in combination with the wishes of the patients. Usually static and hemodynamic imaging are done, however

quality hemodynamic imaging is not always available on short notice as nuclear imaging centers capable of doing hemodynamic imaging are scarce across the world

The PIRAMD score has the potential to structure this workflow and provide a more objective few of Moyamoya. In 2019, another Moyamoya disease scoring system based on TTP changes was introduced by Lin *et al.* (30). He used TTP normalized by the TTP of the cerebellar hemisphere and showed that normalized TTP values could be used to evaluate Moyamoya patients before and after surgery. Although enticing, the use of only one hemodynamic parameter makes the scoring system easy to use, but also is an oversimplification of Moyamoya disease as a complex disease.

Moreover, using the cerebellum especially in case of bilateral disease could severely limit the scoring system in case of crossed cerebellar disease (15,31).

Physiological aspects of Moyamoya disease

Moyamoya can lead to different patterns of brain tissue injury, and can cause recurrent multiple TIAs, cerebral infarction, and intracranial bleeding (1,2). Chronic and recurrent brain structural damage, especially chronic hypoperfusion with chronic ischemia, can result in cortical thinning, which can be assessed with structural MR imaging (22,32). Moreover, impaired vascular reserve and steal phenomenon can aggravate localized brain tissue ischemia, ultimately leading to atrophy and cortical thinning (22,33). Although, chronic structural changes can significantly alter patients' outcome, in everyday clinical practice they are not easy to assess. The presence of prior infarction can be simply evaluated by reviewing the FLAIR/T2 sequences of structural MRI, and is, therefore, an important part of PIRAMD score. Furthermore, presence of prior infracts play an important role regarding decision for surgical revascularization in those patients, as many physicians will be reluctant to decide on surgical revascularization of an asymptomatic patient.

Hemodynamic features of Moyamoya disease

In patients with Moyamoya disease, a progressive narrowing of the supraclinoidal ICA and its proximal branches with development of numerous fragile collateral vessels (1), results in impaired and often paradoxical CVR (i.e., steal phenomenon) (34,35). Vasodilatation of arterioles and collateral flow pathways play important compensatory roles in maintaining regional CBF and tissue viability (36). Since direct CBF measurement methods such as acetazolamide challenged (^{15}O-)H$_2$O-Positron Emission Tomography or ^{133}Xe-Single Photon Emission Computed Tomography lack widespread availability and due to the necessity for a radioactive tracer are very costly (13,37,38), alternative methods have been implemented to measure CBF response to a vasodilatory stimulus, i.e., CVR (34,39,40). A noninvasive BOLD fMRI scan has shown great promise for reproducibly measuring quantitative local and whole brain CVR (23,41), and in comparison to positron emission tomography-CVR showed a good agreement for Moyamoya patients (39,41,42). Due to impaired or even paradoxical vascular reserve, adult Moyamoya patients often present with TIA or ischemic strokes (43). In previous studies, an impaired BOLD-CVR in combination with (recurrent) clinical symptoms, has been used to identify patients who may benefit from surgical revascularization (40,44). Reversal of impaired BOLD-CVR has also been shown to improve the brain structurally (33). Standardized and reproducible BOLD-CVR studies using the RespirAct™ enabled reproducible normoxic hypercapnic stimulus (19,45). In contrast, the stimulus used by Ladner *et al.* (11) was uncontrolled as were the oxygen levels. The reproducible BOLD-CVR measurements enabled a more consistent inter-subject evaluation of the BOLD-CVR maps (46) that was sufficiently robust for comparing subjects across the cohorts. To achieve a similar comparability, Ladner *et al.* (11) attempted to normalization the qualitative CVR maps using the cerebellum as a reference when its CVR is not uniform across patients. This potentially results in suboptimal CVR maps since cerebellar CVR values may be heterogeneous across patients, in particular in the presence of crossed cerebellar diaschisis (31,47).

Angiographic features of Moyamoya disease

Diagnostic DSA remains the preferred imaging technique to demonstrate the characteristics of Moyamoya disease. These primary characteristic is the prominent collateral vascular network, which consist of hypertrophic perforator branches and neoangiogenesis around the circle of Willis (1,2,48). Other collateral pathways occur via pial-to-pial anastomoses from other less compromised territories, or in more advanced cases via dural-pial anastomoses (2,49). Suzuki and Kodama listed 6 angiographic stages of Moyamoya disease that appear with progression of the disease (50). Later, the mSS grading the disease severity into five scores was introduced (44).

The angiographic features presented in this study have been extensively studied in relationship to hemodynamic features. For instance, in previous studies, the presence of cerebrovascular collaterals correlated well with the mSS for disease severity as well as the initial Suzuki score (26,35). The mSS has also been correlated with activation of collateral pathways, specifically leptomeningeal collateralisation has shown to be associated with a higher mSS (26). Recently, the activation of leptomeningeal collateralisation over the posterior circulation has been correlated BOLD-CVR in terms of the extent of reduced CVR and the extent of the region with steal phenomenon (22,23,44,46,47). The improved collateralisation after revascularisation in Moyamoya patients also correlates with improved BOLD-CVR (51). The findings indicate the important role BOLD CVR plays in defining the efficacy of the collateralization response to progressive steno-occlusion. However, in spite of the potential important value of impaired CVR as an individual contributor to the PIRAMD score, the overall score inferred the highest diagnostic correlation.

Advantages and disadvantages of the PIRAMD scoring system

The recently developed PIRAMD score (11) allows for an advanced grading of Moyamoya patients since it incorporates clinical, angiographic, structural and hemodynamic components, and is useful for evaluating patients in need for further management (i.e., revascularization). Our data confirm the usefulness of PIRAMD grades for categorizing hemispheres into asymptomatic and symptomatic. However, the effect of this model on improving treatment outcomes remains to be determined. The high collinearity between CVR and hemodynamic parameters as well as the known influence of revascularization on improving these parameters, indicates that the PIRAMD score should perform well for evaluating the effect of revascularization.

A potential disadvantage of the PIRAMD score is the need for DSA to classify a patient. This limits its use for repeated measurements. A complete assessment using only MR imaging is possible, however, there is only a moderate agreement between MR Angiography and DSA (52,53). However, as an initial assessment and after a revascularization process, the PIRAMD score could prove to be a useful tool.

It could be proposed that as a follow up, only the MR based parameters of the PIRAMD score are repeatedly evaluated. This would result in information about structural changes and hemodynamic changes using BOLD-CVR with information lacking about collateral status. With stabile imaging there is no need for extra angiographic information seeing the extra risk of each additional angiographic. Moreover, statistically there was a high collinearity between the MRI and DSA parameters, this would mean that a stabile MR imaging would infer a stabile angiographic result and follow-up could occur with only MR-based sequencing. In case of a parameter change, the additional DSA can then be performed to create a new PIRAMD score.

As mentioned, BOLD-CVR was obtained using a unique gas delivery system that generates reproducible CO_2 stimuli and, therefore, quantitative BOLD CVR values. Therefore, this technique and gas application is somewhat different from the technique used by Ladner and colleagues. This may have potentially resulted in different CVR findings despite the similar patient cohort. The good agreement found for CVR, though, shows that these small differences do not seem to matter in a disease with large hemodynamic alterations like Moyamoya disease, where significant BOLD-CVR impairment is usually found (i.e., paradoxical BOLD-CVR response/steal phenomenon). If this score also performs well in combination with BOLD-CVR measurements using other vasoactive stimuli, like breath-holding or acetazolamide, is unclear.

Limitations

This is a retrospective analysis of prospectively collected data, similar to the study design by Ladner et al. (11), where the data used was not primarily obtained for this study and therefore there is a time difference between the DSA and the MRI potentially influencing the parameters. Although Moyamoya is a progressive disease, it is unlikely that a 6-week maximum interval between the MRI study and the DSA would cause major structural or hemodynamic changes, although new "silent" infarctions cannot be ruled out.

Last, the PIRAMD score utilizes CVR as binary score (i.e., either impaired or non-impaired). This does not provide information about the extent of hemodynamic disease in a single patient, merely if more then 1/3 of the anterior circulation is affected or not. This could underestimate hemodynamic impairment as severely impaired CVR, but not negative CVR could also be a reason for a symptomatic hemisphere. Moreover, regions with negative CVR <1/3 of the anterior circulation could

still have significant hemodynamic impairment. However, as the extend of hemodynamic impairment is a significant factor in potential surgical treatment of Moyamoya disease, such cut-off value was understandably chosen.

Conclusions

Our multicentric validation of the PIRAMD scoring system was highly effective in scoring the severity of ischemic Moyamoya disease with excellent inter-institutional agreement. Future studies should investigate the prognostic value of this novel imaging-based score in patients with Moyamoya disease.

Acknowledgments

Footnote

Reporting Checklist: The authors have completed the TRIPOD reporting checklist. Available at https://qims.amegroups.com/article/view/10.21037/qims-22-1062/rc

Conflicts of Interest: All authors have completed the ICMJE uniform disclosure form (available at https://qims.amegroups.com/article/view/10.21037/qims-22-1062/coif). JAF and DJM report that they contributed to the development of an automated end-tidal targeting device, RespirActTM which is designed, assembled, and made available as a research tool by Thornhill Medical Inc. (TMI). TMI is a for profit spin-off company from the University Health Network/University of Toronto. JAF and DJM have equity in TMI. The other authors have no conflicts of interest to declare.

Ethical Statement: The authors are accountable for all aspects of the work in ensuring that questions related to the accuracy or integrity of any part of the work are appropriately investigated and resolved. The study was conducted in accordance with the Declaration of Helsinki (as revised in 2013). This study was approved by the ethics committee of University Hospital Zurich (KEK-ZH-Nr. 2012-0427 & KEK 2020-02314) and the research ethics board (UHN REB #13-7168) at the University Health Network of Toronto Western Hospital. All patients signed an informed consent.

Open Access Statement: This is an Open Access article distributed in accordance with the Creative Commons Attribution-NonCommercial-NoDerivs 4.0 International License (CC BY-NC-ND 4.0), which permits the non-commercial replication and distribution of the article with the strict proviso that no changes or edits are made and the original work is properly cited (including links to both the formal publication through the relevant DOI and the license). See: https://creativecommons.org/licenses/by-nc-nd/4.0/.

References

1. Scott RM, Smith ER. Moyamoya disease and moyamoya syndrome. N Engl J Med 2009;360:1226-37.
2. Burke GM, Burke AM, Sherma AK, Hurley MC, Batjer HH, Bendok BR. Moyamoya disease: a summary. Neurosurg Focus 2009;26:E11.
3. Zhu F, Qian Y, Xu B, Gu Y, Karunanithi K, Zhu W, Chen L, Mao Y, Morgan MK. Quantitative assessment of changes in hemodynamics of the internal carotid artery after bypass surgery for moyamoya disease. J Neurosurg 2018;129:677-83.
4. Xu B, Song DL, Mao Y, Gu YX, Xu H, Liao YJ, Liu CH, Zhou LF. Superficial temporal artery-middle cerebral artery bypass combined with encephalo-duro-myo-synangiosis in treating moyamoya disease: surgical techniques, indications and midterm follow-up results. Chin Med J (Engl) 2012;125:4398-405.
5. Kronenburg A, Esposito G, Fierstra J, Braun KP, Regli L. Combined Bypass Technique for Contemporary Revascularization of Unilateral MCA and Bilateral Frontal Territories in Moyamoya Vasculopathy. Acta Neurochir Suppl 2014;119:65-70.
6. Pandey P, Steinberg GK. Neurosurgical advances in the treatment of moyamoya disease. Stroke 2011;42:3304-10.
7. Liu JJ, Steinberg GK. Direct Versus Indirect Bypass for Moyamoya Disease. Neurosurg Clin N Am 2017;28:361-74.
8. Smith ER. Moyamoya arteriopathy. Curr Treat Options Neurol 2012;14:549-56.
9. McKetton L, Venkatraghavan L, Rosen C, Mandell DM, Sam K, Sobczyk O, Poublanc J, Gray E, Crawley A, Duffin J, Fisher JA, Mikulis DJ. Improved White Matter Cerebrovascular Reactivity after Revascularization in Patients with Steno-Occlusive Disease. AJNR Am J Neuroradiol 2019;40:45-50.

10. Han JS, Abou-Hamden A, Mandell DM, Poublanc J, Crawley AP, Fisher JA, Mikulis DJ, Tymianski M. Impact of extracranial-intracranial bypass on cerebrovascular reactivity and clinical outcome in patients with symptomatic moyamoya vasculopathy. Stroke 2011;42:3047-54.

11. Ladner TR, Donahue MJ, Arteaga DF, Faraco CC, Roach BA, Davis LT, Jordan LC, Froehler MT, Strother MK. Prior Infarcts, Reactivity, and Angiography in Moyamoya Disease (PIRAMD): a scoring system for moyamoya severity based on multimodal hemodynamic imaging. J Neurosurg 2017;126:495-503.

12. Sobczyk O, Battisti-Charbonney A, Poublanc J, Crawley AP, Sam K, Fierstra J, Mandell DM, Mikulis DJ, Duffin J, Fisher JA. Assessing cerebrovascular reactivity abnormality by comparison to a reference atlas. J Cereb Blood Flow Metab 2015;35:213-20.

13. Fierstra J, van Niftrik C, Warnock G, Wegener S, Piccirelli M, Pangalu A, Esposito G, Valavanis A, Buck A, Luft A, Bozinov O, Regli L. Staging Hemodynamic Failure With Blood Oxygen-Level-Dependent Functional Magnetic Resonance Imaging Cerebrovascular Reactivity: A Comparison Versus Gold Standard ((15)O-)H(2)O-Positron Emission Tomography. Stroke 2018;49:621-9.

14. van Niftrik CHB, Piccirelli M, Bozinov O, Maldaner N, Strittmatter C, Pangalu A, Valavanis A, Regli L, Fierstra J. Impact of baseline CO(2) on Blood-Oxygenation-Level-Dependent MRI measurements of cerebrovascular reactivity and task-evoked signal activation. Magn Reson Imaging 2018;49:123-30.

15. Sebök M, van Niftrik CHB, Piccirelli M, Muscas G, Pangalu A, Wegener S, Stippich C, Regli L, Fierstra J. Crossed Cerebellar Diaschisis in Patients With Symptomatic Unilateral Anterior Circulation Stroke Is Associated With Hemodynamic Impairment in the Ipsilateral MCA Territory. J Magn Reson Imaging 2021;53:1190-7.

16. Fierstra J, Sobczyk O, Battisti-Charbonney A, Mandell DM, Poublanc J, Crawley AP, Mikulis DJ, Duffin J, Fisher JA. Measuring cerebrovascular reactivity: what stimulus to use? J Physiol 2013;591:5809-21.

17. Sobczyk O, Battisti-Charbonney A, Fierstra J, Mandell DM, Poublanc J, Crawley AP, Mikulis DJ, Duffin J, Fisher JA. A conceptual model for CO -induced redistribution of cerebral blood flow with experimental confirmation using BOLD MRI. Neuroimage 2014;92:56-68.

18. Slessarev M, Han J, Mardimae A, Prisman E, Preiss D, Volgyesi G, Ansel C, Duffin J, Fisher JA. Prospective targeting and control of end-tidal CO2 and O2 concentrations. J Physiol 2007;581:1207-19.

19. van Niftrik CHB, Piccirelli M, Bozinov O, Pangalu A, Fisher JA, Valavanis A, Luft AR, Weller M, Regli L, Fierstra J. Iterative analysis of cerebrovascular reactivity dynamic response by temporal decomposition. Brain Behav 2017;7:e00705.

20. van Niftrik CHB, Piccirelli M, Muscas G, Sebök M, Fisher JA, Bozinov O, Stippich C, Valavanis A, Regli L, Fierstra J. The voxel-wise analysis of false negative fMRI activation in regions of provoked impaired cerebrovascular reactivity. PLoS One 2019;14:e0215294.

21. Sebök M, van Niftrik CHB, Winklhofer S, Wegener S, Esposito G, Stippich C, Luft A, Regli L, Fierstra J. Mapping Cerebrovascular Reactivity Impairment in Patients With Symptomatic Unilateral Carotid Artery Disease. J Am Heart Assoc 2021;10:e020792.

22. Fierstra J, Poublanc J, Han JS, Silver F, Tymianski M, Crawley AP, Fisher JA, Mikulis DJ. Steal physiology is spatially associated with cortical thinning. J Neurol Neurosurg Psychiatry 2010;81:290-3.

23. van Niftrik CHB, Sebök M, Wegener S, Esposito G, Halter M, Hiller A, Stippich C, Luft AR, Regli L, Fierstra J. Increased Ipsilateral Posterior Cerebral Artery P2-Segment Flow Velocity Predicts Hemodynamic Impairment. Stroke 2021;52:1469-72.

24. Sebök M, Esposito G, Niftrik CHBV, Fierstra J, Schubert T, Wegener S, Held J, Kulcsár Z, Luft AR, Regli L. Flow augmentation STA-MCA bypass evaluation for patients with acute stroke and unilateral large vessel occlusion: a proposal for an urgent bypass flowchart. J Neurosurg 2022. [Epub ahead of print]. doi: 10.3171/2021.10.JNS21986.

25. Sebök M, van Niftrik CHB, Wegener S, Luft A, Regli L, Fierstra J. Agreement of novel hemodynamic imaging parameters for the acute and chronic stages of ischemic stroke: a matched-pair cohort study. Neurosurg Focus 2021;51:E12.

26. Strother MK, Anderson MD, Singer RJ, Du L, Moore RD, Shyr Y, Ladner TR, Arteaga D, Day MA, Clemmons PF, Donahue MJ. Cerebrovascular collaterals correlate with disease severity in adult North American patients with Moyamoya disease. AJNR Am J Neuroradiol 2014;35:1318-24.

27. Barber PA, Demchuk AM, Zhang J, Buchan AM. Validity and reliability of a quantitative computed tomography score in predicting outcome of hyperacute stroke before thrombolytic therapy. ASPECTS Study Group. Alberta Stroke Programme Early CT Score. Lancet

2000;355:1670-4.

28. Jaja BNR, Saposnik G, Lingsma HF, Macdonald E, Thorpe KE, Mamdani M, et al. Development and validation of outcome prediction models for aneurysmal subarachnoid haemorrhage: the SAHIT multinational cohort study. BMJ 2018;360:j5745.

29. Steyerberg EW. Clinical Prediction models A practical approach to Development, Validation and Updating: Springer; 2010.

30. Lin YH, Kuo MF, Lu CJ, Lee CW, Yang SH, Huang YC, Liu HM, Chen YF. Standardized MR Perfusion Scoring System for Evaluation of Sequential Perfusion Changes and Surgical Outcome of Moyamoya Disease. AJNR Am J Neuroradiol 2019;40:260-6.

31. Sebök M, van Niftrik CHB, Piccirelli M, Bozinov O, Wegener S, Esposito G, Pangalu A, Valavanis A, Buck A, Luft AR, Regli L, Fierstra J. BOLD cerebrovascular reactivity as a novel marker for crossed cerebellar diaschisis. Neurology 2018;91:e1328-37.

32. Lehman VT, Cogswell PM, Rinaldo L, Brinjikji W, Huston J, Klaas JP, Lanzino G. Contemporary and emerging magnetic resonance imaging methods for evaluation of moyamoya disease. Neurosurg Focus 2019;47:E6.

33. Fierstra J, Maclean DB, Fisher JA, Han JS, Mandell DM, Conklin J, Poublanc J, Crawley AP, Regli L, Mikulis DJ, Tymianski M. Surgical revascularization reverses cerebral cortical thinning in patients with severe cerebrovascular steno-occlusive disease. Stroke 2011;42:1631-7.

34. Sam K, Poublanc J, Sobczyk O, Han JS, Battisti-Charbonney A, Mandell DM, Tymianski M, Crawley AP, Fisher JA, Mikulis DJ. Assessing the effect of unilateral cerebral revascularisation on the vascular reactivity of the non-intervened hemisphere: a retrospective observational study. BMJ Open 2015;5:e006014.

35. Heyn C, Poublanc J, Crawley A, Mandell D, Han JS, Tymianski M, terBrugge K, Fisher JA, Mikulis DJ. Quantification of cerebrovascular reactivity by blood oxygen level-dependent MR imaging and correlation with conventional angiography in patients with Moyamoya disease. AJNR Am J Neuroradiol 2010;31:862-7.

36. Derdeyn CP, Grubb RL Jr, Powers WJ. Cerebral hemodynamic impairment: methods of measurement and association with stroke risk. Neurology 1999;53:251-9.

37. Powers WJ, Zazulia AR. PET in Cerebrovascular Disease. PET Clin 2010;5:83106.

38. Webster MW, Makaroun MS, Steed DL, Smith HA, Johnson DW, Yonas H. Compromised cerebral blood flow reactivity is a predictor of stroke in patients with symptomatic carotid artery occlusive disease. J Vasc Surg 1995;21:338-44; discussion 344-5.

39. Kronenburg A, Bulder MMM, Bokkers RPH, Hartkamp NS, Hendrikse J, Vonken EJ, Kappelle LJ, van der Zwan A, Klijn CJM, Braun KPJ. Cerebrovascular Reactivity Measured with ASL Perfusion MRI, Ivy Sign, and Regional Tissue Vascularization in Moyamoya. World Neurosurg 2019;125:e639-50.

40. Conklin J, Fierstra J, Crawley AP, Han JS, Poublanc J, Mandell DM, Silver FL, Tymianski M, Fisher JA, Mikulis DJ. Impaired cerebrovascular reactivity with steal phenomenon is associated with increased diffusion in white matter of patients with Moyamoya disease. Stroke 2010;41:1610-6.

41. Hendrik Bas van Niftrik C, Sebök M, Muscas G, Piccirelli M, Serra C, Krayenbühl N, Pangalu A, Bozinov O, Luft A, Stippich C, Regli L, Fierstra J. Characterizing ipsilateral thalamic diaschisis in symptomatic cerebrovascular steno-occlusive patients. J Cereb Blood Flow Metab 2020;40:563-73.

42. Hauser TK, Seeger A, Bender B, Klose U, Thurow J, Ernemann U, Tatagiba M, Meyer PT, Khan N, Roder C. Hypercapnic BOLD MRI compared to H(2)(15)O PET/CT for the hemodynamic evaluation of patients with Moyamoya Disease. Neuroimage Clin 2019;22:101713.

43. Hallemeier CL, Rich KM, Grubb RL Jr, Chicoine MR, Moran CJ, Cross DT 3rd, Zipfel GJ, Dacey RG Jr, Derdeyn CP. Clinical features and outcome in North American adults with moyamoya phenomenon. Stroke 2006;37:1490-6.

44. Mesiwala AH, Sviri G, Fatemi N, Britz GW, Newell DW. Long-term outcome of superficial temporal artery-middle cerebral artery bypass for patients with moyamoya disease in the US. Neurosurg Focus 2008;24:E15.

45. Fisher JA, Venkatraghavan L, Mikulis DJ. Magnetic Resonance Imaging-Based Cerebrovascular Reactivity and Hemodynamic Reserve. Stroke 2018;49:2011-8.

46. Kassner A, Winter JD, Poublanc J, Mikulis DJ, Crawley AP. Blood-oxygen level dependent MRI measures of cerebrovascular reactivity using a controlled respiratory challenge: reproducibility and gender differences. J Magn Reson Imaging 2010;31:298-304.

47. von Bieberstein L, van Niftrik CHB, Sebök M, El Amki M, Piccirelli M, Stippich C, Regli L, Luft AR, Fierstra J, Wegener S. Crossed Cerebellar Diaschisis Indicates Hemodynamic Compromise in Ischemic Stroke Patients. Transl Stroke Res 2021;12:39-48.

48. Baltsavias G, Khan N, Valavanis A. The collateral circulation in pediatric moyamoya disease. Childs Nerv Syst 2015;31:389-98.

49. Matsushige T, Kraemer M, Sato T, Berlit P, Forsting M, Ladd ME, Jabbarli R, Sure U, Khan N, Schlamann M, Wrede KH. Visualization and Classification of Deeply Seated Collateral Networks in Moyamoya Angiopathy with 7T MRI. AJNR Am J Neuroradiol 2018;39:1248-54.

50. Suzuki J, Kodama N. Moyamoya disease--a review. Stroke 1983;14:104-9.

51. Watchmaker JM, Frederick BD, Fusco MR, Davis LT, Juttukonda MR, Lants SK, Kirshner HS, Donahue MJ.

Clinical Use of Cerebrovascular Compliance Imaging to Evaluate Revascularization in Patients With Moyamoya. Neurosurgery 2019;84:261-71.

52. Saeki N, Silva MN, Kubota M, Takanashi J, Sugita K, Nakazaki S, Yamaura A. Comparative performance of magnetic resonance angiography and conventional angiography in moyamoya disease. J Clin Neurosci 2000;7:112-5.

53. Song P, Qin J, Lun H, Qiao P, Xie A, Li G. Magnetic Resonance Imaging (MRI) and Digital Subtraction Angiography Investigation of Childhood Moyamoya Disease. J Child Neurol 2017;32:1027-34.